INSTITUT DE FRANCE
Académie des sciences

Comptes Rendus

Physique

Heather Gray and Patrick Janot

Higgs Physics

Volume 21, issue 1 (2020), p. 23-43

Published online: 17 September 2020
Issue date: 17 September 2020

https://doi.org/10.5802/crphys.8

Part of Special Issue: A perspective of High Energy Physics from precision measurements

Guest editors: Stéphane Monteil (Clermont Université, CNRS/IN2P3, Clermont-Ferrand) and Marie-Hélène Schune (Université Paris-Saclay, CNRS/IN2P3, Orsay)

Les Comptes Rendus. Physique *sont membres du Centre Mersenne pour l'édition scientifique ouverte*
www.centre-mersenne.org
e-ISSN : 1878-1535

Comptes Rendus
Physique
2020, 21, nº 1, p. 23-43
https://doi.org/10.5802/crphys.8

A perspective of High Energy Physics from precision measurements
La physique des Hautes Energies du point de vue des mesures de précision

Higgs Physics

La Physique du Boson de Higgs

Heather Gray[a] **and Patrick Janot**[*, b]

[a] Department of Physics, University of California, Berkeley, CA 94720, USA

[b] CERN, 1 Esplanade des Particules, CH-1217 Meyrin, Switzerland.

E-mails: heather.gray@berkeley.edu (H. Gray), patrick.janot@cern.ch (P. Janot).

Abstract. The existence of the Higgs boson was postulated more than 50 years ago, without any indication of its mass. The quest that followed, with several generations of particle physics experiments, culminated with the recent discovery of a new particle with a mass of 125 GeV. At least another half-century will be needed to map the properties of this particle with sufficient precision to understand its deepest origin.

Résumé. L'existence du boson de Higgs a été postulée il y a plus de 50 ans sans indication d'un ordre de grandeur pour sa masse. La longue recherche qui s'en suivit, impliquant plusieurs générations d'expériences de physique des particules a été enfin couronnée par la découverte récente d'une nouvelle particule de masse de 125 GeV. Il s'en faudra sans doute de cinquante années supplémentaires pour en découvrir les propriétés avec une précision suffisante pour comprendre la profonde origine physique de cette particule.

Keywords. Higgs, Discovery, Properties, Future, Colliders, New physics.

Mots-clés. Higgs, Découverte, Propriétés, Futur, Collisionneurs, Nouvelle physique.

1. Introduction

The Higgs mechanism [1–4] was proposed in 1964 as a theoretical way to provide mass to the gauge bosons, through their interactions with the Higgs field, while safeguarding the symmetries believed to underlie modern particle physics. This vital development enabled Glashow [5], Weinberg [6], and Salam [7] to independently propose a unified "electroweak" theory, with a massless photon for the electromagnetic interaction, and massive Z and W bosons for the weak interaction. In a summary talk for the ICHEP conference in 1974, John Iliopoulos presented, for the first time in a single report [8], the view of physics now called the Standard Model (SM). When applied in the SM, the Higgs mechanism predicts the existence of a scalar particle, the Higgs boson H, which directly couples to SM particles – including itself – proportionally to their masses, but with an unknown mass, m_H.

* Corresponding author.

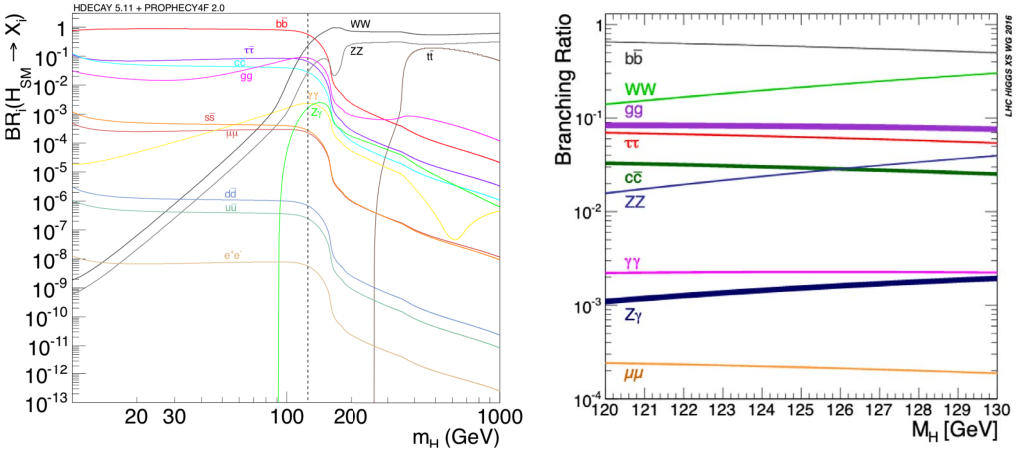

Figure 1. Predicted decay branching ratios of the SM Higgs boson over a wide mass range (left [9]) and close-up around $m_H = 125$ GeV (right [10]).

For any value of m_H, the production cross sections and decay rates of the SM Higgs boson can therefore be calculated accurately. For illustration, the predicted branching fractions are displayed in Figure 1 as a function of its mass. A campaign of searches for the SM Higgs boson was deployed over the following 50 years. This story, summarised in Section 2, culminated at LHC in 2012 with the discovery of a particle with a mass of 125 GeV, and with properties consistent with expectations for the SM Higgs boson.

With this discovery, the spectrum of particles and the interactions described by the SM are complete. Particle physics, however, must continue its investigations. On the one hand, many theoretical and experimental questions remained unanswered; on the other, the properties of the discovered particle are far from having been measured with the same precision as those of the other SM particles. It is essential to determine these properties with an accuracy order(s) of magnitude better than today, and to acquire sensitivity to the processes that, during the time span from 10^{-12} to 10^{-10} seconds after the Big Bang, led to the formation of today's Higgs vacuum field. Future hadron and lepton colliders are proposed to do exactly that. Their capabilities are reviewed and contrasted in Sections 3 to 5. Conclusions are offered in Section 6.

2. Current status of Higgs Physics

2.1. *Situation before LHC*

The first searches for a massless or light SM Higgs boson were performed in nuclear transitions and neutron-nucleon scattering [11, 12] in the early 1970s. They were followed in the 1980s by searches in the decays of pions [13], kaons [14], B mesons [15], J/ψ's and Υ's [16] (with a Higgs boson decay into e^+e^- or $\mu^+\mu^-$) as discussed in Ref. [17], and a search by an original beam-dump experiment [18]. By 1989, a massless Higgs boson, and a Higgs boson with mass between 1 and 110 MeV, were excluded. A Higgs boson with a mass below 5–6 GeV was considered very unlikely, but not firmly excluded due to theoretical loopholes [17].

In the 20 years that followed, searches for a heavier Higgs boson were performed at the Large Electron-Positron collider (LEP) [19], located at CERN (Geneva, Switzerland) and at the Tevatron [20], located at Fermilab (Chicago, Illinois), benefiting from its large and unambiguously known couplings to the Z and the W. At LEP, electrons and positrons collided at a centre-of-mass

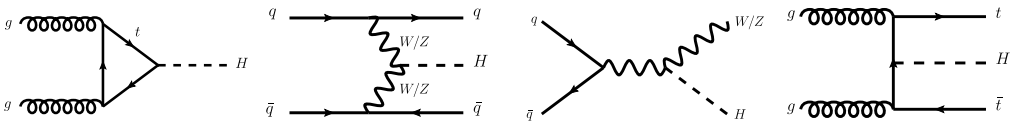

Figure 2. Higgs production modes with the largest cross section at LHC. From left to right, the production modes are gluon-gluon fusion; vector boson fusion; associated production with a vector boson; and associated production with a pair of top quarks.

energy around the Z pole until 1995 (LEP1) and up to 209 GeV from 1996 to 2000 (LEP2). The Tevatron began colliding protons and anti-protons in 1985 initally at $\sqrt{s} = 1.8$ TeV and then from 2002 to 2011 at $\sqrt{s} = 1.96$ TeV.

Direct searches at LEP were performed using the Higgsstrahlung process, $e^+e^- \to HZ^{(*)}$, with the Z decaying to a pair of charged leptons, neutrinos, or quarks. By the end of the LEP1 period, no such events had been found, and the mass range from 0.0 GeV to 65.6 GeV was excluded from these direct searches [21]. By the end of LEP2, a small excess of events was observed around 115 GeV in the last year of operation, and the lower limit on m_H increased to 114.4 GeV [22]. Indirect effects of the Higgs boson on electroweak precision observables were also measured at LEP1, with almost 20 million recorded Z decays. In combination with the direct determination of the W and top masses at the Tevatron, these electroweak precision measurements constrained the SM Higgs boson mass in the range from 54 to 132 GeV [23]. Together with direct searches, the region between 114.4 and 132 GeV was thus favoured in the SM framework, at the 95% confidence level.

Direct searches for the SM Higgs boson produced in association with a vector boson, $q\bar{q} \to WH$ and ZH, were performed at the Tevatron. A small excess of events was found between 115 and 140 GeV, i.e. in the region still allowed by LEP precision measurements and direct searches, and Higgs boson masses between 149 and 182 GeV were excluded [24].

2.2. *Higgs discovery and measurements at LHC*

The Large Hadron Collider (LHC) [25] began colliding protons in 2009, reusing the existing LEP tunnel at CERN. At LHC, the most copious Higgs production mode is gluon-gluon fusion with a cross section of 17 pb at $\sqrt{s} = 7$ TeV [10]. Ordered by decreasing cross section, this mode is followed by vector boson fusion; associated production with a W or Z boson; and associated production with a pair of top quarks; as illustrated in Figure 2. A wide range of decay modes are accessible ranging from the high-resolution and low-background decays to four leptons (via ZZ^* decay) and a pair of photons, through WW^* and $\tau^+\tau^-$ decays, all the way to the low-resolution and high-background $b\bar{b}$ decay.

By the end of 2011, the ATLAS and CMS collaborations had collected approximately 5 fb^{-1} of data at a centre-of-mass energy of 7 TeV. After all channels had been analysed and combined, the SM Higgs boson was excluded for all masses except for a small range around 125 GeV, where a modest excess of events with a significance of 2 to 3σ was observed by each experiment [26,27].

In 2012, the centre-of-mass energy increased from 7 to 8 TeV and the dataset doubled to 10 fb^{-1} by the summer. At a joint seminar on 4 July 2012, the ATLAS and CMS collaborations reported the observation of a narrow resonance with a mass of approximately 126 GeV with statistical significance of 5.0σ and 4.9σ respectively [28, 29] and subsequently published this result in Refs. [30, 31]. Figure 3 shows two of the distributions contributing to this observation: $H \to ZZ^* \to 4\ell$ from ATLAS and $H \to \gamma\gamma$ from CMS.

Since the discovery in 2012, many of the properties of this new resonance have been measured and, so far, all these properties are consistent with the predictions for the SM Higgs boson. The

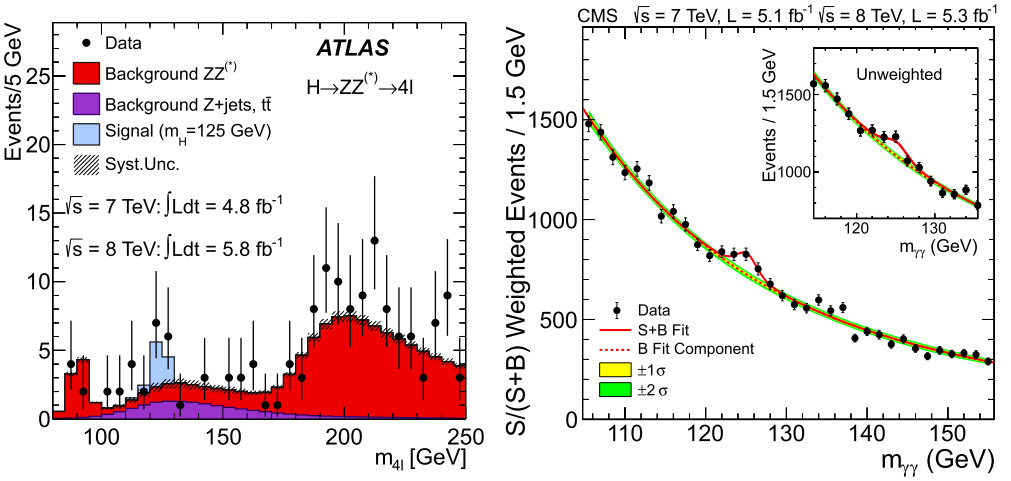

Figure 3. The invariant mass distribution in the 4ℓ channel from the CMS experiment using 10.5 fb^{-1} of data (left). The invariant mass distribution in the diphoton channel from the ATLAS experiment using 10.4 fb^{-1} of data (right). From Refs. [30, 31].

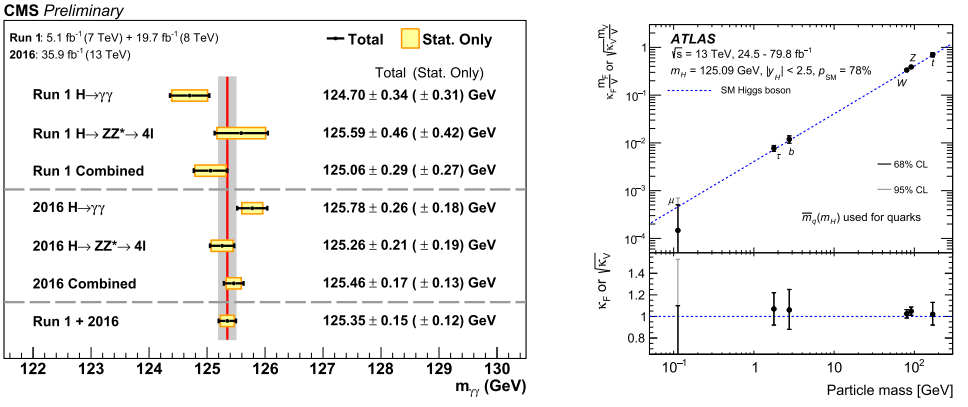

Figure 4. (Left) Summary of the measurements from the CMS experiment of the Higgs mass using the $H \to ZZ^* \to 4\ell$ and the $H \to \gamma\gamma$ channels. Results using data from Run1 and Run2 and their combination are shown. The total uncertainty is indicated in black and the systematic uncertainty in yellow. From Ref. [34]. The reduced coupling strength for fermions and bosons to the Higgs boson as a function of the particle mass from the ATLAS experiment using data recorded at 13 TeV. The blue dashed line is indicative of the prediction from the SM for either fermions or bosons. From Ref. [35].

mass is obtained by fitting the invariant mass in the $H \to ZZ^* \to 4\ell$ and $H \to \gamma\gamma$ channels, and was measured to be $m_H = 125.09 \pm 0.21(\text{stat.}) \pm 0.11(\text{syst.})$ [32] in the combination of the ATLAS and CMS measurements using the approximately 25 fb^{-1} of data from Run1, which occurred from 2010 to 2012. Between 2015 and 2018, Run2 followed with a centre-of-mass energy of 13 TeV. The current measurements of the Higgs mass are $m_H = 124.97 \pm 0.24$ GeV [33] and $m_H = 125.35 \pm 0.15$ GeV [34] for ATLAS and CMS respectively using both Run1 and Run2 data. Figure 4 summarises the measurements of the Higgs mass made by the CMS experiment for each channel and each dataset. The $H \to ZZ^* \to 4\ell$ is statistically limited, but the $H \to \gamma\gamma$ measurement has statistical and systematic uncertainties of comparable size.

The Standard Model predicts that the width of a Higgs boson with mass of 125 GeV is 4.2 MeV [10]. Because hadron colliders can only measure the product of the production cross section and the branching ratio, the total width cannot be inferred without assumptions (see Section 4 for a discussion about the Higgs width measurement at lepton colliders). Direct measurements, e.g. from the width of the invariant mass distribution in the $H \to ZZ^* \to 4\ell$ channel, are sensitive to widths of 1–2 GeV, three orders of magnitude larger than the SM prediction. Indirect constraints on the width can be set by measuring the ratio of the cross section of on-shell (around the Higgs mass) to off-shell (higher invariant masses) Higgs production in vector boson decay channels [36–39]. These measurements of the off-shell production rate can also be used to set limits on the anomalous couplings of the Higgs boson.

The SM Higgs boson is predicted to have a zero total angular momentum, positive parity and positive charge parity. Due to the observation of the $H \to \gamma\gamma$ decay, the charge parity is known to be positive. The angular momentum and parity have been probed by measuring the angular distributions of the decay products on the Higgs boson using the $H \to \gamma\gamma$, $H \to WW^*$ and $H \to ZZ^*$ decays. The spin and parity measurements are independent of the measurements of the total rate in each channel. Constraints on the spin and CP of the Higgs boson have also been set using the $H \to \tau^+\tau^-$ decay channels [40, 41].

Under certain assumptions, these results can be translated into model-dependent measurements of the coupling of the Higgs boson to the other SM particles as shown in Figure 4. (This model dependence can be lifted with the absolute measurement of the HZZ coupling at a lepton collider, as explained in Section 4.) All major production modes have been observed. The cross section for Higgs production through gluon-gluon fusion has been measured to a precision of 10% [35, 42, 43] and the observation of the production of the Higgs boson in association with top quarks, with a cross section two orders of magnitude smaller was made by both ATLAS and CMS in 2018 [44, 45]. The strength of the coupling between the Higgs boson and the top quark is in agreement with indirect measurements. The decay of the Higgs boson has been observed in the following five channels: $H \to \gamma\gamma$, $H \to ZZ^* \to 4\ell$, $H \to WW^*$, $H \to \tau^+\tau^-$ and $H \to b\bar{b}$. The most recent observation has been the decay of the Higgs boson to bottom quarks in 2018 [46, 47]. No significant deviations from SM predictions have been observed in either the production or the decay modes.

The growing LHC dataset has also been used to set limits on channels with much smaller branching ratios. For example, the upper limit on the Higgs branching ratio to $Z\gamma$ is currently 1.4 times the SM prediction [48, 49]. So far, no observation has been made of the coupling of the Higgs bosons to fermions outside the third generation. The most promising channel, $H \to \mu\mu$, allowed an upper limit of 1.7 times the SM to be set [50, 51]. Searches for the decay of the Higgs boson to charm quarks have also been performed, but current limits are more than an order of magnitude above the SM prediction [52, 53].

The measurement of the self-coupling of the Higgs boson will be a key physics target for HL-LHC as discussed in Section 3.1, but searches for Higgs pair production (HH) are already being performed at LHC. A large number of final states are required to cover the different possible decay combinations of the two Higgs bosons. At LHC, the most sensitive modes are $HH \to b\bar{b}\tau^+\tau^-$ and $HH \to b\bar{b}\gamma\gamma$. The current observed (expected) upper limits on the Higgs pair production cross section are 6.9 (10) for ATLAS [54] and 12.8 (22.3) for CMS [55] times the SM prediction.

2.3. *Searches for Higgs Physics beyond the Standard Model*

The Higgs boson could be a portal to new physics in many ways. Selected examples are provided to illustrate the type of constraints obtained at LHC on Higgs physics beyond the Standard Model.

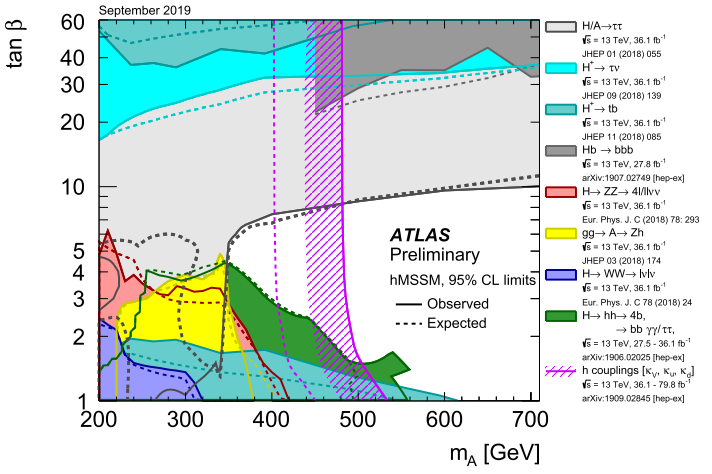

Figure 5. Regions of the $(m_A, \tan\beta)$ plane in the MSSM excluded by searches for additional Higgs bosons. Results from direct searches are indicated with solid shading and results from indirect searches are indicated with hatched shading. From Ref. [58].

Decays of the Higgs boson can be used to search for new particles with masses less than half that of the Higgs boson, either with direct searches or via a combined fit to all coupling measurements. Under the assumption that the Higgs couplings to the Z and the W are not larger than the SM prediction, ATLAS and CMS constrained the branching ratio of the Higgs boson to invisible or undetected particles, $\mathscr{B}_{\text{inv}}$, to be less than 34% [32]. Direct searches from ATLAS and CMS in the VBF production mode led to similar upper limits of $\mathscr{B}_{\text{inv}} < 37\%$ [56] and $\mathscr{B}_{\text{inv}} < 33\%$ [57].

Additional Higgs bosons can be searched for at LHC over a wide mass range in many decay channels. In minimal nonminimal versions of the Standard Model, two Higgs doublets are introduced to give mass to up-type and down-type quarks separately. In these models, the Higgs sector consists of five physical states: three neutral Higgs bosons (the SM-like Higgs boson h; another, heavier, CP-even state H; and a CP-odd state A), and a pair of charged Higgs bosons ($H^{\pm}$). The ratio of the vacuum expectations of the two Higgs doublets is denoted $\tan\beta$.

Figure 5 shows regions of the $(m_A, \tan\beta)$ plane in the minimal supersymmetric extension of the SM (MSSM), excluded by searches for such additional Higgs bosons. Direct searches have excluded high and low values of $\tan\beta$ and with the mass of one of the charged Higgs bosons, m_A, required to be above 350 GeV. Indirect limits from coupling fits are shown in pink and exclude m_A below 500 GeV [58].

3. Higgs Physics at future hadron colliders

The highest energy elementary parton–parton collisions can be achieved, for the foreseeable future, with high-energy proton–proton colliders, for which a circular geometry is the only available option, at least for energies up to ≈150 TeV. In the LHC tunnel, the High-Luminosity LHC (HL-LHC) [59] will have a collision energy of 14 TeV and a luminosity 5 to 7 times larger than that of LHC. Three other hadron colliders are currently under study. The High-Energy LHC (HE-LHC) [60] would still use the LHC tunnel with upgraded dipole magnets, to reach a energy of 27 TeV. The FCC-hh [61] would collide protons at a centre-of-mass energy of at least 100 TeV in a new tunnel with a circumference of 100 km near CERN. A similar infrastructure, called Super

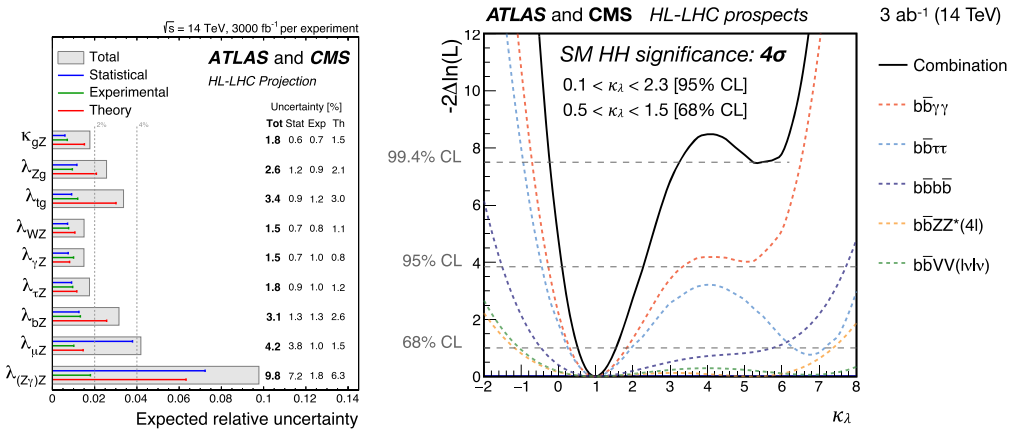

Figure 6. (Left) The expected uncertainty on the ratios of Higgs coupling modifiers, κ, from the combination of ATLAS and CMS at HL-LHC showing separately the statistical, experimental and theoretical uncertainties from Ref. [63]. (Right) The expected precision on the Higgs self-coupling, κ_λ from HL-LHC shown as the minimum negative-log-likelihood distribution from the combination of all channels for ATLAS and CMS using the full HL-LHC dataset from Ref. [63]. The likelihoods for the individual channels are also shown.

proton–proton Collider (SppC [62]) is also proposed in China. In this note, the capabilities for Higgs physics of HL-LHC and FCC-hh are discussed.

3.1. *The luminosity frontier: HL-LHC*

The HL-LHC is expected to begin operation after 2027 to provide 3 ab^{-1} of data. The large data sample will improve the precision of many LHC measurements, and open up new possibilities inaccessible at LHC.

The left panel of Figure 6 shows the expected uncertainty on the ratio of Higgs coupling modifiers, κ, with respect to the coupling of the Higgs boson to the Z boson [63]. Projections are shown from the combination of the ATLAS and CMS results with the full dataset expected at HL-LHC. For many channels, HL-LHC measurements are expected to reach a precision better than 2%, typically dominated by theoretical uncertainties. Rare Higgs decays such as $H \to Z\gamma$ and $H \to \mu\mu$ are expected to be measured to a precision of 9.8% and 4.2% respectively. Under the assumption that $\kappa_{W,Z} \leq 1$, HL-LHC will be able to probe invisible and undetected decays of the Higgs boson with a precision of a few percent.

The HL-LHC is also expected to provide the first evidence for the Higgs self-coupling with the measurement of the Higgs pair inclusive and differential cross sections. The right panel of Figure 6 shows the expected precision on the Higgs self-coupling for the combination of ATLAS and CMS, with the full expected HL-LHC dataset. The expected significance from the combination of all channels and both experiments is 4σ [63] and the most sensitive channel is $b\bar{b}\gamma\gamma$ [63].

3.2. *The energy frontier: FCC-hh*

One of the key physics targets of FCC-hh will be studying the nature of the Higgs potential by measuring Higgs pair production with high precision. The leading order diagrams for Higgs

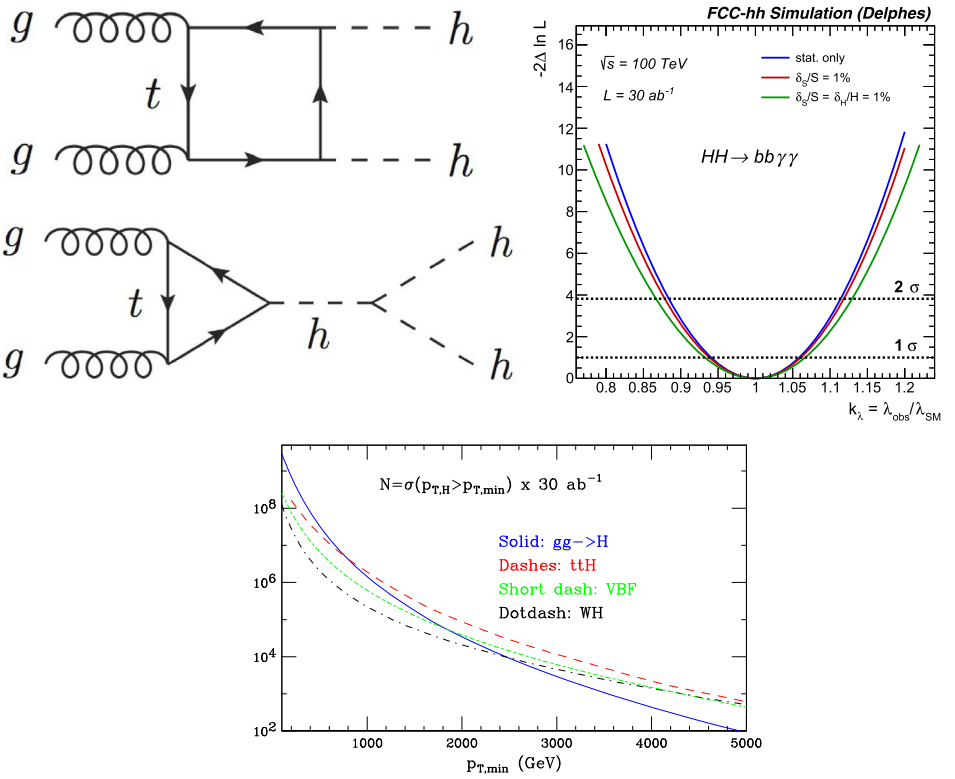

Figure 7. (Top left) Leading order Feynman diagrams for Higgs pair production at pp colliders. (Top right) The expected precision on the Higgs self-coupling from FCC-hh in the $H \to b\bar{b}\gamma\gamma$ channel. The negative log-likelihood curves are shown for statistical uncertainties only (blue) and then under different assumptions on the systematic uncertainties (red, green). (Bottom) The number of Higgs bosons that are expected to be produced at FCC-hh as a function of the transverse momentum of the Higgs boson for various production modes. From Ref. [64].

pair production are shown in the upper-left panel of Figure 7. The lower diagram is the one sensitive to the Higgs self-coupling, while the upper diagram shows the most important SM background. The two diagrams have strong negative interference, which means that the cross section is very small and the accuracy of the measurement relies on both the high-energy and the high-luminosity of the collider. One of the most powerful channels to probe this coupling at FCC-hh will be the $HH \to b\bar{b}\gamma\gamma$ decay channel. The upper-right panel of Figure 7 shows the negative log-likelihood for this channel that is expected at FCC-hh, corresponding to an expected precision on κ_λ of 6.5% [64]. A recent combination with other final states ($b\bar{b}\gamma\gamma$, $b\bar{b}\tau^+\tau^-$, $b\bar{b}b\bar{b}$, and $b\bar{b}ZZ$) improves the expected precision further, leading to a target of 3 to 4.5% on κ_λ [65].

The 3×10^{10} Higgs bosons that could be produced at FCC-hh would improve the precision of certain measurements and open up the possibility of new measurements. The transverse momentum distribution for the Higgs boson in a variety of production modes is shown in the lower panel of Figure 7. The many thousands of Higgs boson with momentum about 2 TeV will be produced in each of the production modes. This can be exploited at FCC-hh to measure ratios of Higgs coupling by selecting events with large transverse momentum which significantly reduces

Table 1. The expected FCC-hh precision on ratios of Higgs branching ratios and the branching ratio to invisible particles. From Ref. [64]

Observable	Precision (stat)	Precision (stat + syst + lumi)
$B(H \to \mu\mu)/B(H \to 4\mu)$	0.33%	1.3%
$B(H \to \gamma\gamma)/B(H \to 2e2\mu)$	0.17%	0.8%
$\sigma(t\bar{t}H) \times B(H \to b\bar{b})/\sigma(t\bar{t}Z) \times B(Z \to b\bar{b})$	1.05%	1.9%
$B(H \to \text{invisible})$	1×10^{-4}	2.5×10^{-4}

the backgrounds. In addition, the transverse momentum of the Higgs boson can be measured to search for contributions from new physics processes. Table 1 shows that the expected precision for the $H \to \mu\mu$ and $H \to \gamma\gamma$ channels would be approximately 1%. The coupling of the Higgs boson to top quarks can be measured to 1% accuracy by measuring the ratio of $t\bar{t}H$ to $t\bar{t}Z$ production. By fitting the missing energy distribution, FCC-hh could probe the branching ratio of the Higgs boson to invisible and undetected decay to the 10^{-4} level. Further details about these studies are available in Ref. [64].

4. Higgs Physics at future lepton colliders

In the present state of strategic discussions, a consensus emerges around the strong physics case for an e^+e^- collider at the precision frontier, to measure the Higgs boson and the other particle properties with unprecedented accuracy. At the time of writing, four e^+e^- collider projects are still on the table [66–72]. The physics case is summarised in the Physics Briefing Book [73].

The circular colliders (FCC-ee and CEPC) were conceived in 2011–2013, as soon as first hints for a light Higgs boson became publicly known [74]. Their luminosity curves provides the highest statistics at low energies, but is strongly limited by synchrotron radiation above 350–400 GeV. The proposed operation models comprise data taking at and around the Z pole (91 GeV), at the WW threshold (161 GeV), at the ZH cross-section maximum (240 GeV), and, for FCC-ee, an extension at and above the top pair threshold (up to 365 GeV). The designs are sufficiently flexible to allow operation at other centre-of-mass energies (e.g., at $\sqrt{s} = m_H$, or well below the Z peak), with unrivalled luminosities. Both colliders are planned to operate for 10–15 years with two IPs (A configuration with four IPs is being studied for FCC-ee.), and are considered to be a first, enabling step in a long-term plan towards a high-energy proton–proton collider (Section 3.2).

Linear colliders have been studied since 1975 [75], and are considered to be the only possible way towards higher-energy e^+e^- collisions. The luminosity and power consumption grows linearly with energy. The proposed operation models include a first run at "low" energy, 250 GeV for ILC and 380 GeV for CLIC, for about a decade. Both colliders have an open-ended run plan, with possible extensions to 1 TeV (ILC) and 3 TeV (CLIC) in a run plan that extends over several decades.

At the top-pair threshold, FCC-ee, CLIC, and ILC are planned to deliver similar integrated luminosities, within a factor of two. A linear collider is the most effective option at 500 GeV (and the only possibility for higher energies), while a circular collider is more effective for any energy below 350–400 GeV. For example, at the ZH cross-section maximum, FCC-ee is expected to produce 5 ab^{-1} in about three years, while it would take between 20 and 30 years with ILC to reach the same figure. The integrated power for a circular machine is also five to ten times less per Higgs boson produced at the ZH cross-section maximum.

In the longer term, $\mu^+\mu^-$ collisions could also be envisioned [76–78], once the considerable technological challenges related to muon production, cooling, acceleration, and decay backgrounds, have been solved. The reduced synchrotron radiation loss from muons – by a factor 10^9

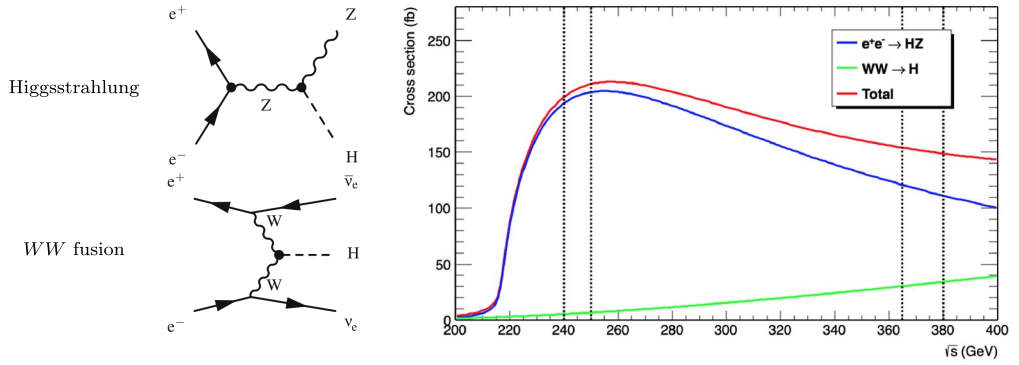

Figure 8. (Left) Feynman diagrams for the Higgsstrahlung (top) and the WW fusion (bottom) processes. (Right) Unpolarised Higgs production cross section as a function of the centre-of-mass energy $\sqrt{s}$. Vertical dashed lines indicate the values of $\sqrt{s}$ foreseen for the four low-energy Higgs factories: FCC-ee (240 and 365 GeV), CEPC (240 GeV), ILC (250 GeV) and CLIC (380 GeV).

with respect to electrons – would then enable the construction of circular colliders either with much smaller radii at low energies, or with much higher design energies, typically 6 to 14 TeV. Possible operation models include a low-energy run at $\sqrt{s} = m_H$, in a ring of a few 100 m circumference, benefiting from a larger coupling to the Higgs boson and an exquisite energy definition; followed by multi-TeV collisions, e.g., in the LEP/LHC ring.

4.1. *The luminosity frontier: low-energy Higgs factories*

In e^+e^- collisions at centre-of-mass energies from 240 to 380 GeV, the two main Higgs production mechanisms are the Higgsstrahlung process, $e^+e^- \to ZH$, and the WW fusion process, $e^+e^- \to H\nu_e\bar{\nu}_e$, with Feynman diagrams and cross sections shown in Figure 8. With the integrated luminosities foreseen to be accumulated by each of the four colliders, over one million Higgs bosons would be collected at FCC-ee and CEPC, about 500,000 at ILC, and less than 200,000 at CLIC.

The total ZH cross section, proportional to the Higgs coupling to the Z boson g^2_{HZZ}, can be determined in a model-independent manner by counting events with an identified Z (decaying into e^+e^- or $\mu^+\mu^-$, for example), and for which the mass m_R recoiling against the Z, given by $m_R^2 = s + m_Z^2 - 2\sqrt{s}(E_{\ell^+} + E_{\ell^-})$, clusters around 125 GeV. This absolute measurement of g_{HZZ}, unique to e^+e^- colliders, can be used as a "standard candle" by all other measurements, including those made at HL-LHC and FCC-hh. The position of the recoil mass peak also provides an accurate measurement of the Higgs boson mass. Once g_{HZZ} has been determined, the measurement of the cross sections for each exclusive Higgs boson decay, $H \to X\overline{X}$,

$$\sigma_{ZH} \times \mathscr{B}(H \to X\overline{X}) \propto \frac{g^2_{HZZ} \times g^2_{HXX}}{\Gamma_H} \quad \text{and} \quad \sigma_{H\nu_e\bar{\nu}_e} \times \mathscr{B}(H \to X\overline{X}) \propto \frac{g^2_{HWW} \times g^2_{HXX}}{\Gamma_H}, \qquad (1)$$

gives access to all other couplings in a model-independent, absolute, way. For example, the ratio of the WW-fusion-to-Higgsstrahlung cross sections for the same Higgs boson decay, proportional to g^2_{HWW}/g^2_{HZZ}, yields g_{HWW}, and the Higgsstrahlung rate with the $H \to ZZ$ decay, proportional to g^4_{HZZ}/Γ_H, provides a determination of the Higgs boson total decay width. The precision with which the Higgs mass, width and couplings can be measured at the various e^+e^- colliders is given

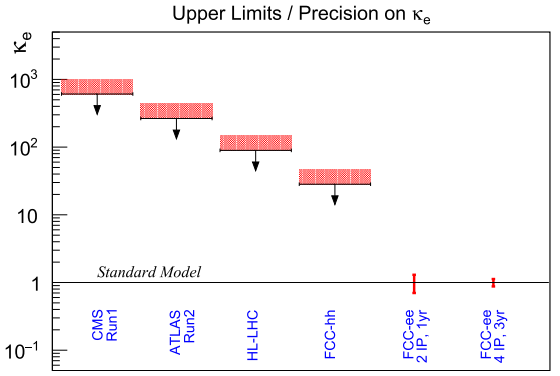

Figure 9. Current upper limits on the Higgs boson coupling modifier to electrons, κ_e, from CMS [80] and ATLAS [81]; projected κ_e upper limits at HL-LHC and FCC-hh; and projected κ_e precisions at FCC-ee in two different running configurations (one year with 2 IPs, or three years with 4 IPs).

in Section 5. The longitudinal beam polarisation, available at linear colliders, plays little role in this determination [68].

Several Higgs boson couplings, however, are not directly accessible from its decays, either because the masses involved, and therefore the decay branching ratios, are too small to allow for an observation within 10^6 events or less – as is the case for the couplings to the particles of the first SM family: electron, up quark, down quark – or because the masses involved are too large for the decay to be kinematically open – as is the case for the top-quark Yukawa coupling and for the Higgs boson self coupling. Other methods are therefore required, as described below.

The ability of FCC-ee to provide the highest luminosities at lower centre-of-mass energies offers the unique opportunity to measure the Higgs boson coupling to electrons through the resonant production process $e^+e^- \to H$ at $\sqrt{s} = 125$ GeV [79]. A 2σ excess (with respect to a situation in which the Higgs boson does not couple to electrons) would be observed at FCC-ee after a year with two interaction points, and a precision of ±15% on the Higgs boson coupling to the electron can be observed after three years with four interaction points. A comparison with the hadron collider sensitivity is displayed in Figure 9.

The Higgs self-coupling can be obtained by two different methods [82]. The method with single Higgs production [83] at low-energy Higgs factories relies on the precise measurement of the ZH cross section, which depends on the self-coupling via the diagrams shown in the left panel of Figure 10. This measurement provides a robust self-coupling determination from at least two sufficiently different energy points [84–86], e.g., 240 and 365 GeV. A precision of ±34% on the self-coupling can be achieved at FCC-ee (right panel of Figure 10), reduced to ±24% with four IPs instead of two [87]. No meaningful constraint can obtained with only a single centre-of-mass energy. The first 4σ demonstration of the existence of the Higgs self-coupling is therefore within reach in 15 years at FCC-ee.

Finally, the top Yukawa coupling will have been determined with a few percent precision – albeit with some model dependence – at HL-LHC, well before the advent of any e^+e^- collider. The model-dependence of the HL-LHC measurement will be lifted off by the g_{HZZ} absolute measurement made at low-energy Higgs factories. As mentioned in Section 3.2, the measurement of the ttZ coupling (for example at FCC-ee$_{365}$ [88]) and the measurement of the cross section ratio $\sigma_{ttH}/\sigma_{ttZ}$ at FCC-hh will provide another significant improvement in precision for the top Yukawa coupling, to better than ±1%.

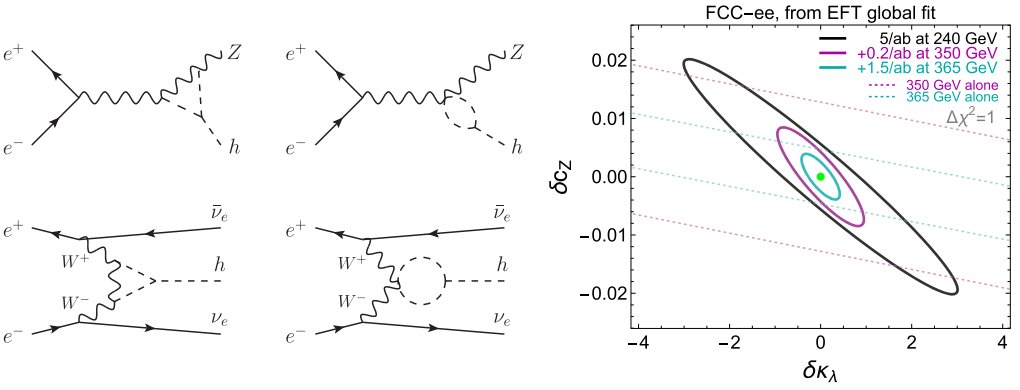

Figure 10. Left, from Ref. [84]: sample Feynman diagrams illustrating the effects of the Higgs self-coupling on single Higgs process at next-to-leading order. Right: FCC-ee precision in the simultaneous determination of the Higgs self-coupling κ_λ and the HZZ/HWW coupling c_Z, at 240 GeV (black ellipse), 350 GeV (purpled dashed), 365 GeV (green dashed), and by combining data at 240 and 350 GeV (purple ellipse), and at 240, 350, and 365 GeV (green ellipse).

All the above could in principle also be achieved with a low-energy muon collider ring of only 600 m circumference. The luminosity at a centre-of-mass energy of 240–250 GeV, however, is expected to be 10 (100) times smaller than at a linear (circular) e^+e^- collider. This configuration is therefore inadequate for precision measurements of Higgs properties in any reasonable time. Interestingly, the resonant process $\mu^+\mu^- \to H$ at $\sqrt{s} = 125$ GeV has a cross section $\sim 40{,}000$ times larger than its e^+e^- counterpart. Between 5,000 and 15,000 Higgs bosons could be produced every year in a scan of the Higgs lineshape. Such a scan does not provide a "standard candle" to hadron colliders, and is not competitive for the Higgs coupling precision, but it would be the only possibility to reveal substructure in the lineshape, e.g., due to two Higgs bosons almost degenerate in mass. In conclusion, a muon circular collider at $\sqrt{s} = 125$ GeV would be an elegant Higgs factory, but not necessarily the one needed for precision measurements (and therefore, for sensitivity to new physics).

4.2. *The energy frontier: Higgs physics at $\sqrt{s} \geq 500$ GeV*

4.2.1. *Study of the H(125) properties*

With their open-ended energy-upgrade plan, linear colliders progressively produce a larger number of Higgs bosons in the WW-fusion process and reach one million Higgs bosons after two or three additional decades of operation at 0.5 (1) TeV for ILC, and 1.5 (3) TeV for CLIC, with integrated luminosities of 4 (8) and 2.5 (5) ab^{-1}, respectively.

New Higgs production processes become available when the centre-of-mass energy exceeds 500 GeV, as shown in Figure 11. For example, the ttH and ZHH cross sections are just sufficient at 500 GeV (~100 ab) to enable independent measurements of the top Yukawa coupling and of the Higgs self-coupling with precisions of ±6% and ±27%, respectively. A slight increase of the centre-of-mass energy to 550 GeV would improve the top Yukawa coupling precision to ±4%, which would make ILC_{500} competitive with HL-LHC and FCC-ee for these two couplings. For these essential measurements, having both FCC-ee and ILC_{500} (or even better, ILC_{600} to get close to the maximum of the ZHH, ttH, and ttZ cross sections) would provide important verification in case a discrepancy with the SM predictions is found, and improved precision altogether –

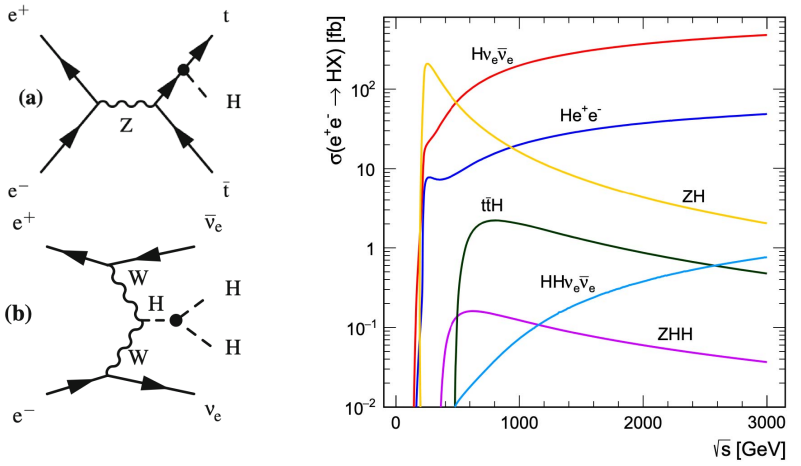

Figure 11. (Left) Feynman diagrams of the leading-order processes involving (a) the top Yukawa coupling g_{Htt}, and (b) the Higgs boson self-coupling g_{HHH}. (Right) Unpolarised production cross sections for the main Higgs production processes up to $\sqrt{s} = 3$ TeV. From Ref. [72].

i.e., new physics sensitivity to higher mass scale – with a combination of both sets of data. It is only with the highest energies and the full luminosity that $\text{ILC}_{1\,\text{TeV}}$ and $\text{CLIC}_{3\,\text{TeV}}$ would offer a precision of about ±10% on the Higgs self-coupling, with an analysis of the $HH\nu_e\bar{\nu}_e$ process.

At FCC, the current baseline strategy to access to double Higgs production is to not upgrade the energy FCC-ee to 500 GeV, but to move to proton–proton collisions at the much higher energy of 100 TeV (see Section 3.2). It has been recently realised, however, that FCC-ee could be, as an intermediate step towards FCC-hh, upgraded with the Energy-Recovery Linacs (ERL) technology, to reach an energy of 600 GeV with a luminosity 5 to 50 ab^{-1} in 10 years of operation with one interaction point [89]. With such a luminosity, up to ten times that expected at a linear collider at the same energy, a measurement of the Higgs self-coupling with a 10% precision can be contemplated as well. Needless to say, the level of understanding of such a possibility is nowhere near that of the ILC or CLIC designs, and will require in depth feasibility and cost studies, comparable to that made for the well-established baseline ring-ring design at lower energies, to fully validate the concept.

4.2.2. *Search for additional Higgs states*

The new states in two-Higgs-doublet models, H, A, and $H^{\pm}$ can searched for with lepton colliders through their production in pairs: e^+e^- or $\mu^+\mu^- \to HA$ or H^+H^-, with a sensitivity for discovery up to $\sqrt{s}/2$. The added value of a high-energy muon collider would be twofold in this respect. Firstly, the potentially higher centre-of-mass energy (up to 14 TeV) allows the pair production to be sensitive to additional Higgs states with masses up to 7 TeV. Secondly, the large $H\mu\mu$ coupling opens the possibility of an automatic mass scan of the neutral states up to $m_{H,A} = \sqrt{s}$, with the "radiative return" process: $\mu^+\mu^- \to H\gamma$ or $A\gamma$ [90]. For $\sqrt{s} = 3$ TeV, events selected with an isolated photon of energy above 10 GeV would have a recoil-mass distribution as displayed in the left panel of Figure 12, pointing clearly to the mass of a new neutral Higgs state. The collider centre-of-mass energy would then be tuned to the new state mass, in order to copiously produce both CP-even and CP-odd state through resonant production: $\mu^+\mu^- \to H,\ A$, as displayed in the right panel of Figure 12 [91], providing a unique laboratory for H/A mixing and CP violation studies [92].

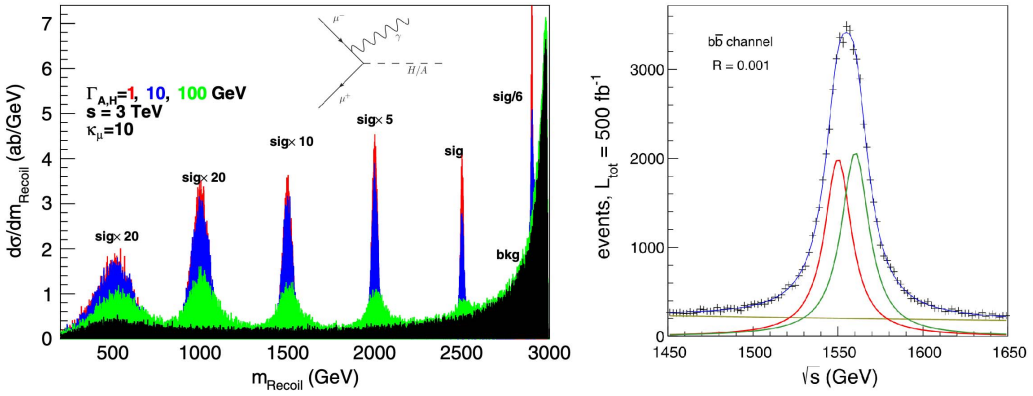

Figure 12. (Left, from Ref. [90]) Distribution of the mass recoiling against an isolated photon with momentum transverse to the beam in excess of 10 GeV, for heavy Higgs (H, A) masses of 0.5, 1, 1.5, 2, 2.5, and 2.9 TeV, with total width of 1 (red), 10 (blue), and 100 (green) GeV, at a 3 TeV muon collider. The beam energy resolution is assumed to amount to 0.1%. Signal and backgrounds have different multiplication factors for clarity. (Right, from Ref. [91]) Scan of the H/A lineshape ($m_{H,A} \sim 1.55$ TeV) in the $\mu^+\mu^- \to b\bar{b}$ production with $\sqrt{s}$ from 1.45 to 1.65 TeV, with a centre-of-mass energy spread of 0.001 and a total luminosity of 0.5 ab^{-1}.

5. Projected results in κ and EFT fits: discussion

In the SM, the Higgs boson coupling to a given particle X, denoted g_{HXX}, is uniquely fixed by its mass. The quantitative effect of new physics on these couplings requires a parametrisation of the induced deviations with respect to the SM predictions. Two such parametrisations are widely used, the κ framework; and the effective field theory (EFT) approach.

The simpler κ framework introduces multiplicative modifiers $\kappa_X = g_{HXX}/g^{\rm SM}_{HXX}$, for each of the tree-level couplings to SM particles, κ_Z, κ_W, κ_b, κ_c, κ_τ, κ_μ, and κ_t; and three effective modifiers for the loop-induced couplings, κ_γ, κ_g, and $\kappa_{Z\gamma}$; and one resulting modifier for the Higgs decay width, κ_H. The couplings κ_s, κ_d, κ_u and κ_e, that are only weakly constrained from very rare decays, are currently not included in the combined κ-framework fits. The κ-framework also allows for the possibility of Higgs boson decays to invisible or "untagged" BSM particles, with the introduction of two additional branching ratio parameters, $\mathscr{B}_{\rm inv}$ and $\mathscr{B}_{\rm EXO}$. For colliders that can directly measure the Higgs width (such as FCC-ee), $\mathscr{B}_{\rm EXO}$ can be constrained together with κ_X and $\mathscr{B}_{\rm inv}$ from a combined fit to the data. For colliders that cannot (such as HL-LHC), additional theoretical assumptions must be introduced (for example by fixing the width and other couplings to their SM prediction). The κ framework makes no assumption on the new physics that modifies the couplings. Constraints derived in the κ analysis can therefore be readily exploited to derive model-independent constraints on the new physics parameters. In certain new physics model, however, the κ framework is sub-optimal in setting constraints, as it is blind to effects that do not change the coupling strengths, but change instead their helicity structure (which would modify, e.g., angular distributions).

To circumvent this shortcoming, the EFT approach is introduced to parametrise directly the new physics (rather than its effects) in terms of gauge invariant operators of dimension 6, 8, 10, etc, and calculated through an expansion in inverse powers of the new-physics mass scale Λ. Current EFT approaches typically only consider the supposedly dominant $\mathscr{O}(1/\Lambda^2)$ terms, carried by dimension-six operators. While more sensitive than the κ framework to new physics effects,

Table 2. Precision on the Higgs boson couplings g_{HXX}, from Ref. [82] in the κ framework (left) and in a global EFT fit to Higgs, diboson, and electroweak precision measurements (right), for the five low-energy Higgs factories (μColl$_{125}$, ILC$_{250}$, CLIC$_{380}$, CEPC$_{240}$, and FCC-ee$_{240\to365}$), fixing the Higgs self-coupling g_{HHH} to its SM value. For the g_{HHH} fit, only the EFT global fit result is shown (with 2IPs and 4IPs for FCC-ee). For the muon collider, only the results of a standalone κ fit are displayed. All numbers are in % and indicate 68% C.L. sensitivities. Also indicated in the κ fit are the precision on the total decay width and the 95% C.L. sensitivity on the "invisible" and "exotic" branching fractions

Collider	HL-LHC	μColl$_{125}$	ILC$_{250}$	CLIC$_{380}$	CEPC$_{240}$	FCC-ee$_{240\to365}$
Lumi (ab^{-1})	3	0.005	2	1	5.6	5 + 0.2 + 1.5
Years	10	6 to 10	11.5	8	7	3 + 1 + 4
g_{HZZ} (%)	1.5/3.6	SM	0.29/0.39	0.44/0.50	0.18/0.45	0.17/0.26
g_{HWW} (%)	1.7/3.2	3.9	1.0/0.41	0.73/0.50	0.88/0.43	0.41/0.27
g_{Hbb} (%)	3.7/5.3	3.8	1.1/0.78	1.2/0.99	0.92/0.63	0.64/0.56
g_{Hcc} (%)	SM/SM	SM	2.0/1.8	4.1/4.0	2.0/1.8	1.3/1.2
g_{Hgg} (%)	2.5/2.3	SM	1.4/1.1	1.5/1.3	1.0/0.76	0.89/0.82
$g_{H\tau\tau}$ (%)	1.9/3.4	6.2	1.1/0.81	1.4/1.3	0.91/0.66	0.66/0.57
$g_{H\mu\mu}$ (%)	4.3/5.5	3.6	4.2/4.1	4.4/4.4	3.9/3.8	3.9/3.8
$g_{H\gamma\gamma}$ (%)	1.8/3.6	SM	1.4/1.3	1.4/1.4	1.3/1.3	1.3/1.2
$g_{HZ\gamma}$ (%)	10./11.	SM	10./9.6	10./9.7	6.3/6.3	10./9.3
g_{Htt} (%)	3.4/3.5	SM	3.1/3.2	3.2/3.2	3.1/3.1	3.1/3.1
g_{HHH} (%)	50.	SM	49.	50.	49.	33./24.
Γ_H (%)	SM	6.1	2.2	2.5	1.7	1.1
$\mathscr{B}_{\text{inv}}$ (%)	1.9	SM	0.26	0.63	0.27	0.19
$\mathscr{B}_{\text{EXO}}$ (%)	SM (0.0)	SM (0.0)	1.8	2.7	1.1	1.0

this approach needs to make a number of assumptions on the underlying new physics. First, new physics is assumed to be heavy for the $1/\Lambda^n$ expansion to make sense, which excludes a whole class of new physics models that include light particles. Second, new physics must be described by only one mass scale – a criterion that is not satisfied by the standard model. Third, it is assumed that Λ is large enough for dimension-six operators to dominate over all other operators, which restricts EFT analyses to an effective Lagrangian truncated to $1/\Lambda^2$ terms. Last by not least, only a small subset of the 2499 dimension-six operators is assumed to affect Higgs measurements and is included in EFT Higgs analyses. The physics implications of these strong assumptions are not transparent. It can be anticipated that further work will be needed for the Higgs analyses, similar to what was done at LEP to express the measurements in an observable-based, model-independent framework.

Projections have been obtained for both approaches in the context of the Symposium for the European Strategy Update in Granada, in May 2019. Updated results can be found in Ref. [82], and are displayed in Table 2 for Higgs coupling precisions at the different low-energy Higgs factories, when combined with the projected HL-LHC precisions [63]. The Higgs capabilities of their energy-frontier upgrades, still combined with the HL-LHC projections, are compared in Table 3. Such studies do not exist yet for a high-energy muon collider. After completion of their proposed operation models (up to 365 GeV for FCC-ee, up to 1 TeV for ILC, and up to 3 TeV for CLIC), a substantial part of the e^+e^- collider Higgs physics programs is similar. There are, however, significant differences due to the variation of the production mode as a function of energy. Several remarks are in order.

Table 3. Precision on the Higgs boson couplings, from Ref. [82] in the κ framework (left) and in a global EFT fit (right), for the combination of each low-energy Higgs factory (ILC_{250}, $CLIC_{380}$, and FCC-ee) and their proposed upgrades at higher energies: $ILC_{500\,GeV}$, $ILC_{500+1000\,GeV}$, $CLIC_{1.4+3\,TeV}$, and the complete FCC integrated programme. All numbers are in % and indicate 68% C.L. sensitivities. Also indicated are the precision on the total decay width, and the 95% C.L. sensitivity on the "invisible" and "exotic" branching fractions. A precision similar to that achieved at high-energy linear colliders is reached with FCC-hh in less than one year of operation for all couplings, except the Higgs self-coupling for which a precision of 10% is reached in about 3 to 5 years [65] (with respect to a couple decades for ILC_{1000} and CLIC)

Collider	ILC_{500}	ILC_{1000}	CLIC	FCC
g_{HZZ} (%)	0.23/0.22	0.23/0.16	0.39/0.16	0.16/0.13
g_{HWW} (%)	0.29/0.22	0.24/0.17	0.38/0.15	0.19/0.13
g_{Hbb} (%)	0.56/0.52	0.47/0.43	0.53/0.38	0.48/0.44
g_{Hcc} (%)	1.2/1.2	0.90/0.88	1.4/1.4	0.96/0.95
g_{Hgg} (%)	0.85/0.79	0.63/0.55	0.86/0.75	0.50/0.49
$g_{H\tau\tau}$ (%)	0.64/0.58	0.54/0.49	0.82/0.73	0.46/0.46
$g_{H\mu\mu}$ (%)	3.9/3.9	3.6/3.5	3.5/3.5	0.43/0.42
$g_{H\gamma\gamma}$ (%)	1.2/1.2	1.1/1.1	1.2/1.1	0.31/0.34
$g_{HZ\gamma}$ (%)	10./6.8	10./6.7	5.7/3.7	0.70/0.70
g_{Htt} (%)	2.8/2.9	1.4/1.5	2.1/2.1	0.96/1.6
g_{HHH} (%)	27./27.	10/10	9./n.a.	3./4.
Γ_H (%)	1.1	1.0	1.6	0.91
$\mathscr{B}_{\text{inv}}$ (%)	0.23	0.22	0.61	0.024
$\mathscr{B}_{\text{EXO}}$ (%)	1.4	1.4	2.4	1.0

(i) Circular colliders operating at the maximum of the ZH cross section are very efficient Higgs factories, requiring for example ~9 (5) GJ per Higgs boson for FCC-ee with 2 (4) IPs at 240 GeV, vs ~50 GJ for the proposed ILC run plan at 250 GeV. The measurement of the total ZH cross section at FCC-ee provides the most precise determination of the g_{HZZ} coupling. Linear colliders running at higher energies progressively obtain better measurement of g_{HWW} from the $H\nu_e\bar{\nu}_e$ cross section. The synergistic combination of a circular and a linear colliders offers the best test of the SM relationship between the Higgs couplings to the W and Z boson, i.e., a test of the SU(2) custodial symmetry in the Higgs sector. The full integrated FCC (ee-hh-eh) could achieve this test with a similar precision.

(ii) Proton–proton collisions are qualitatively and quantitatively more effective to study the Higgs boson thoroughly at high energy, once the g_{HZZ} and ttZ couplings are determined in an absolute manner by (an) e^+e^- collider(s) operating at 240 GeV and above 350 GeV, respectively, and used as standard candles in pp collisions. The FCC integrated plan yields precision consistently smaller than 1% for all the couplings to gauge bosons and to fermions shown in Table 3, for the invisible and exotic branching fractions, and for the Higgs boson total width. With 5×10^{10} Higgs bosons produced, FCC-hh also gives the most sensitive measurements of the rare decays such as $\mu\mu, \gamma\gamma, Z\gamma$, and of the invisible width.

(iii) The Higgs self-coupling can be obtained by two different methods, as discussed in Ref. [82]. The method with single Higgs production relies on the precise measurement of the ZH cross section, and provides a robust determination from at least two sufficiently

different energy points [86]. The need for these two energies is satisfied by the current operation model of FCC-ee, but also provides a clear opportunity for a synergistic combination of a circular collider (operating up to 240 GeV) and a linear collider (operating above 350 GeV) [93].

(iv) A more precise determination of the Higgs self-coupling, to ±10%, can be obtained either with higher-energy e^+e^- collisions from double Higgs production, at and above the ZHH cross-section maximum – or at high-energy hadron colliders. This is the realm of excellence of ILC at 1 TeV or CLIC at 3 TeV, but could also be achieved with an upgrade of FCC-ee based on Energy Recovery Linacs. A precision of ±3% is possible at FCC-hh, which enjoys a wider phase space for double-Higgs production. For this important measurement, the different sources of systematic uncertainties in e^+e^- and pp collisions would also render their combination more robust than each individual result.

(v) On the other side of the spectrum, FCC-ee offers the unique opportunity to measure the Higgs boson coupling to electrons through the resonant production process $e^+e^- \to H$ at $\sqrt{s} = 125$ GeV [79]. A precision of ±15% on the Higgs boson SM coupling to the electron can be observed after three years with four interaction points. Because of the need of extremely high luminosity, combined with monochromatisation and continuous ppm centre-of-mass energy control, such a measurement is not possible with linear colliders. It is also out of reach of hadron colliders.

In summary, circular colliders provide both the highest luminosity and the best energy efficiency in e^+e^- collisions for $\sqrt{s}$ up to 400 GeV, and the only possibility to deliver proton–proton collisions at 100 TeV and beyond. This interplay is essential for a broad spectrum of unique Higgs measurement, and makes the FCC complex a formidable tool of investigation. The combined sensitivity of FCC-ee and FCC-hh to deviations in the SM couplings and self-coupling, and to the production of new particles coupled to the Higgs, is a portal to physics beyond the SM, and can conclusively test the nature of the cosmological electroweak phase transition [64].

6. Outlook and conclusion

Particle physics has arrived at an important moment of its history. Half a century after having been proposed on purely theoretical grounds, the recent discovery of the Higgs boson with a mass of 125 GeV at LHC, exactly in the range from 114.4 to 132 GeV predicted by LEP and Tevatron precision measurements, completed the spectrum of particles and their interactions, which have constituted the Standard Model for several decades. This model has now become a consistent and predictive theory, which has so far proven successful in describing all phenomena accessible to collider experiments. In particular, today's measurements of the Higgs boson properties are consistent, within still large uncertainties, with the SM expectations.

This achievement does not stop the need for further exploration. Many questions remain unanswered, with the deep origin of the Higgs boson very high on the list. Is the Higgs boson an elementary particle, or is it a composite state of confined particles? What mechanism generates its mass and self-interaction, leading to electroweak symmetry breaking and to the generation of particle masses? What was the nature of the phase transition that led, in the early Universe, to electroweak symmetry breaking? Addressing these questions requires a detailed cartography of the Higgs boson and of the electroweak interactions above the weak scale, with the best possible precision to expose new dynamics.

High-energy lepton and hadron colliders are unique tools to study the Higgs boson in a controlled environment. The cornerstone of the Higgs measurement programme is the direct and model-independent determination of its coupling to the Z boson. This measurement, unique to lepton colliders, is optimally performed at $\sqrt{s}$ around 240 GeV. The measurement of the $H \to ZZ^*$

decay then provide the total Higgs width. Absolute values of the other Higgs couplings follow, and can be done best with a high-energy hadron collider.

There is no doubt that a worldwide plan including both a lepton and a hadron collider will pose considerable challenges, but it would offer the particle physics community complementary and synergistic programs with a long-term vision, as well as answers to the fundamental questions that the discovery of the Higgs boson has brought to the forefront.

References

[1] F. Englert, R. Brout, "Broken symmetry and the mass of gauge vector mesons", *Phys. Rev. Lett.* **13** (1964), no. 9, p. 321-323.

[2] P. W. Higgs, "Broken symmetries, massless particles and gauge fields", *Phys. Lett.* **12** (1964), no. 2, p. 132-133, https://cds.cern.ch/record/641590.

[3] P. W. Higgs, "Broken symmetries and the masses of gauge bosons", *Phys. Rev. Lett.* **13** (1964), p. 508-509.

[4] G. S. Guralnik, C. R. Hagen, T. W. B. Kibble, "Global conservation laws and massless particles", *Phys. Rev. Lett.* **13** (1964), no. 20, p. 585-587.

[5] S. L. Glashow, "Partial symmetries of weak interactions", *Nucl. Phys.* **22** (1961), no. 4, p. 579-588.

[6] S. Weinberg, "A model of leptons", *Phys. Rev. Lett.* **19** (1967), no. 21, p. 1264-1266.

[7] A. Salam, "Weak and Electromagnetic Interactions", *Conf. Proc. C* **680519** (1968), p. 367-377.

[8] J. Iliopoulos, "Progress in Gauge Theories", in *Proceedings, 17th International Conference of High Energy Physics (ICHEP), London, England, July 01–July 10, 1974*, 1974, p. III.89, http://inspirehep.net/record/3000/files/c74-07-01-p089.pdf.

[9] D. d'Enterria, "On the Gaussian peak of the product of decay probabilities of the standard model Higgs boson at a mass $m_H \sim 125$ GeV", 2012, preprint, https://arxiv.org/abs/1208.1993.

[10] D. de Florian *et al.*, "Handbook of LHC Higgs Cross Sections: 4. Deciphering the Nature of the Higgs Sector", 2016, preprint, https://arxiv.org/abs/1610.07922.

[11] D. Kohler, B. A. Watson, J. A. Becker, "Experimental search for a low-mass scalar boson", *Phys. Rev. Lett.* **33** (1974), p. 1628-1631.

[12] R. Barbieri, T. Ericson, "Evidence against the existence of a low mass scalar boson from neutron-nucleus scattering", *Phys. Lett. B* **57** (1975), no. 3, p. 270-272.

[13] SINDRUM collaboration, S. Egli *et al.*, "Measurement of the decay $\pi^+ \to e^+\nu_e e^+e^-$ and search for a light Higgs boson", *Phys. Lett. B* **222** (1989), p. 533-537.

[14] G. D. Barr *et al.*, "Search for a neutral Higgs particle in the decay sequence $K_L^0 \to \pi^0 H^0$ and $H^0 \to e^+e^-$", *Phys. Lett. B* **235** (1989), no. 3-4, p. 356-362, https://cds.cern.ch/record/203195.

[15] CLEO collaboration, M. S. Alam *et al.*, "Search for a Neutral Higgs Boson in *B* Meson Decay", *Phys. Rev. D* **40** (1989), p. 712-720.

[16] CUSB collaboration, J. Lee-Franzini *et al.*, *Proc. of the XXIVth Int. Conf. of High Energy Physics, Munich, Germany, August, 1988*, 1988.

[17] M. Drees *et al.*, "Higgs search at LEP", in *LEP Physics Workshop Geneva, Switzerland, February 20, 1989*, 1989, p. 59.

[18] M. Davier, H. Nguyen Ngoc, "An unambiguous search for a light Higgs boson", *Phys. Lett. B* **229** (1989), p. 150-155.

[19] R. Aßmann, M. Lamont, S. Myers, "A brief history of the LEP collider", *Nucl. Phys. B Proc. Suppl.* **109** (2002), p. 17-31.

[20] H. T. Edwards, "The Tevatron energy doubler: a superconducting accelerator", *Ann. Rev. Nucl. Part. Sci.* **35** (1985), p. 605-660.

[21] P. Janot, "Searching for Higgs bosons at LEP1 and LEP2", in *Advanced Series on Directions in High Energy Physics*, World Scientific, Dec., 1997, p. 104-130.

[22] LEP Working Group for Higgs boson searches, ALEPH, DELPHI, L3, OPAL collaboration, R. Barate *et al.*, "Search for the standard model Higgs boson at LEP", *Phys. Lett. B* **565** (2003), p. 61-75.

[23] J. Haller *et al.*, "Update of the global electroweak fit and constraints on two-Higgs-doublet models", *Eur. Phys. J. C* **78** (2018), article ID 675.

[24] CDF, D0 collaboration, T. Aaltonen *et al.*, "Higgs boson studies at the Tevatron", *Phys. Rev. D* **88** (2013), article ID 052014.

[25] L. Evans, "The large hadron collider", *Ann. Rev. Nucl. Part. Sci.* **61** (2011), p. 435-466.

[26] ATLAS Collaboration, "Combined search for the Standard Model Higgs boson using up to 4.9 fb^{-1} of *pp* collision data at $\sqrt{s} = 7$ TeV with the ATLAS detector at the LHC", *Phys. Lett. B* **710** (2012), no. 1, p. 49-66.

[27] CMS Collaboration, "Combined results of searches for the standard model Higgs boson in *pp* collisions at $\sqrt{s} = 7$ TeV", *Phys. Lett. B* **710** (2012), p. 26-48.

[28] F. Gianotti, "Status of Standard Model Higgs Searches in ATLAS", 2012, *CERN Seminar*, https://indico.cern.ch/event/197461/contributions/1478916/attachments/290953/406671/ATLAS_Higgs-CERN-seminar-2012.pdf.

[29] J. Incandela, "Status of the CMS SM Higgs Search", 2012, *CERN Seminar*, https://indico.cern.ch/event/197461/contributions/1478917/attachments/290954/406673/CMS_4July2012_Final.pdf.

[30] ATLAS Collaboration, "Observation of a new particle in the search for the Standard Model Higgs boson with the ATLAS detector at the LHC", *Phys. Lett. B* **716** (2012), no. 1, p. 1-29.

[31] CMS Collaboration, "Observation of a new boson at a mass of 125 GeV with the CMS experiment at the LHC", *Phys. Lett. B* **716** (2012), no. 1, p. 30-61.

[32] ATLAS and CMS Collaborations, "Combined Measurement of the Higgs Boson Mass in pp Collisions at $\sqrt{s} = 7$ and 8 TeV with the ATLAS and CMS Experiments", *Phys. Rev. Lett.* **114** (2015), no. 19, article ID 191803.

[33] ATLAS Collaboration, "Measurement of the Higgs boson mass in the $H \to ZZ^* \to 4\ell$ and $H \to \gamma\gamma$ channels with $\sqrt{s} = 13$ TeV pp collisions using the ATLAS detector", *Phys. Lett. B* **784** (2018), p. 345-366.

[34] CMS Collaboration, "A measurement of the Higgs boson mass in the diphoton decay channel", Tech. Report CMS-PAS-HIG-19-004, CERN, Geneva, 2019.

[35] ATLAS Collaboration, "Combined measurements of Higgs boson production and decay using up to 80 fb^{-1} of proton-proton collision data at $\sqrt{s} = 13$ TeV collected with the ATLAS experiment", (2019), https://arxiv.org/abs/1909.02845, preprint.

[36] N. Kauer, G. Passarino, "Inadequacy of zero-width approximation for a light Higgs boson signal", *JHEP* **08** (2012), article ID 116.

[37] F. Caola, K. Melnikov, "Constraining the Higgs boson width with ZZ production at the LHC", *Phys. Rev. D* **88** (2013), article ID 054024.

[38] J. M. Campbell, R. K. Ellis, C. Williams, "Bounding the Higgs width at the LHC using full analytic results for $gg \to \text{e}^-\text{e}^+\,\mu^-\,\mu^+$", *JHEP* **04** (2014), article ID 60.

[39] J. M. Campbell, R. K. Ellis, C. Williams, "Bounding the Higgs width at the LHC: complementary results from $H \to WW$", *Phys. Rev. D* **89** (2014), article ID 053011.

[40] ATLAS Collaboration, "Test of *CP* Invariance in vector-boson fusion production of the Higgs boson using the *Optimal Observable* method in the ditau decay channel with the ATLAS detector", *Eur. Phys. J. C* **76** (2016), article ID 658.

[41] CMS Collaboration, "Constraints on anomalous *HVV* couplings from the production of Higgs bosons decaying to τ lepton pairs", *Phys. Rev. D* **100** (2019), article ID 112002.

[42] CMS Collaboration, "Measurements of properties of the Higgs boson in the four-lepton final state in proton-proton collisions at $\sqrt{s} = 13$ TeV", Tech. Report CMS-PAS-HIG-19-001, CERN, 2019, preprint.

[43] CMS Collaboration, "Measurements of Higgs boson production via gluon fusion and vector boson fusion in the diphoton decay channel at $\sqrt{s} = 13$ TeV", Tech. Report CMS-PAS-HIG-18-029, CERN, 2019, preprint.

[44] CMS collaboration, A. M. Sirunyan *et al.*, "Observation of $\text{t}\bar{\text{t}}\text{H}$ production", *Phys. Rev. Lett.* **120** (2018), article ID 231801.

[45] ATLAS Collaboration, "Observation of Higgs boson production in association with a top quark pair at the LHC with the ATLAS detector", *Phys. Lett. B* **784** (2018), p. 173-191.

[46] ATLAS Collaboration, "Observation of $H \to b\bar{b}$ decays and *VH* production with the ATLAS detector", *Phys. Lett. B* **786** (2018), p. 59-86.

[47] CMS Collaboration, "Observation of Higgs boson decay to bottom quarks", *Phys. Rev. Lett.* **121** (2018), article ID 121801.

[48] CMS Collaboration, "Search for the decay of a Higgs boson in the $\ell\ell\gamma$ channel in proton–proton collisions at $\sqrt{s} = 13$ TeV", *JHEP* **11** (2018), article ID 152.

[49] ATLAS Collaboration, "Searches for the $Z\gamma$ decay mode of the Higgs boson and for new high-mass resonances in pp collisions at $\sqrt{s} = 13$ TeV with the ATLAS detector", *JHEP* **10** (2017), article ID 112.

[50] ATLAS Collaboration, "A search for the dimuon decay of the Standard Model Higgs boson in pp collisions at $\sqrt{s} = 13$ TeV with the ATLAS Detector", Tech. Report ATLAS-CONF-2019-028, CERN, Geneva, Jul 2019.

[51] CMS Collaboration, "Search for the Higgs Boson Decaying to Two Muons in Proton–Proton Collisions at $\sqrt{s} = 13$ TeV", *Phys. Rev. Lett.* **122** (2019), article ID 021801.

[52] ATLAS Collaboration, "Search for the decay of the Higgs boson to charm quarks with the ATLAS experiment", *Phys. Rev. Lett.* **120** (2018), article ID 211802.

[53] CMS Collaboration, A. M. Sirunyan *et al.*, "A search for the standard model Higgs boson decaying to charm quarks", *JHEP* **03** (2020), article ID 131.

[54] ATLAS Collaboration, G. Aad *et al.*, "Combination of searches for Higgs boson pairs in pp collisions at $\sqrt{s} = 13$ TeV with the ATLAS detector", *Phys. Lett. B* **800** (2020), article ID 135103.

[55] CMS Collaboration, "Combination of searches for Higgs boson pair production in proton–proton collisions at $\sqrt{s} = 13$ TeV", *Phys. Rev. Lett.* (2018), https://arxiv.org/abs/1811.09689.

[56] ATLAS Collaboration, "Search for invisible Higgs boson decays in vector boson fusion at $\sqrt{s} = 13$ TeV with the ATLAS detector", *Phys. Lett. B* **793** (2019), p. 499-519.

[57] CMS Collaboration, A. M. Sirunyan *et al.*, "Search for invisible decays of a Higgs boson produced through vector boson fusion in proton–proton collisions at $\sqrt{s} = 13$ TeV", *Phys. Lett. B* **793** (2019), p. 520-551.

[58] ATLAS Collaboration, "HBSM working group hMSSM summary plots", ATL-PHYS-PUB-2019-034 (2019).
[59] A. G. *et al.*, "High-Luminosity Large Hadron Collider (HL-LHC): Technical Design Report V. 0.1", 2017, CERN Yellow Reports: Monographs, CERN, Geneva, https://cds.cern.ch/record/2284929.
[60] FCC collaboration, A. Abada *et al.*, "HE-LHC: the high-energy large hadron collider volume", *Eur. Phys. J. ST* **228** (2019), p. 1109-1382.
[61] FCC collaboration, A. Abada *et al.*, "FCC-hh: the hadron collider", *Eur. Phys. J. ST* **228** (2019), p. 755-1107.
[62] C. S. Group, "CEPC Conceptual Design Report: Volume 1 - Accelerator", 2018, preprint, https://arxiv.org/abs/1809.00285.
[63] M. Cepeda *et al.*, "Report from Working Group 2", *CERN Yellow Rep. Monogr.* **7** (2019), p. 221.
[64] FCC collaboration, A. Abada *et al.*, "FCC physics opportunities", *Eur. Phys. J. C* **79** (2019), article ID 474.
[65] M. Selvaggi, "The Higgs self-coupling at FCC-hh", in *3rd FCC Physics and Experiments Workshop, January, 2020,* 2020, https://indico.cern.ch/event/838435/contributions/3635737/attachments/1970292/3277240/HH_fccphysicsWS.pdf.
[66] A. Abada *et al.*, "FCC physics opportunities", *Eur. Phys. J. C* **79** (2019), article ID 474.
[67] A. Abada *et al.*, "FCC-ee: the lepton collider", *Eur. Phys. J. Special Topics* **228** (2019), p. 261-623.
[68] N. A. Tehrani *et al.*, "FCC-ee: your questions answered", in *CERN Council Open Symposium on the Update of European Strategy for Particle Physics (EPPSU) Granada, Spain, May 13–16, 2019* (A. Blondel, P. Janot, eds.), 2019.
[69] CEPC Study Group collaboration, M. Dong *et al.*, "CEPC Conceptual Design Report: Volume 2 - Physics & Detector", 2018, preprint, https://arxiv.org/abs/1811.10545.
[70] K. Fujii *et al.*, "Physics case for the international linear collider", 2015, preprint, https://arxiv.org/abs/1506.05992.
[71] K. Fujii *et al.*, "Physics case for the 250 GeV stage of the international linear collider", 2017, preprint, https://arxiv.org/abs/1710.07621.
[72] H. Abramowicz *et al.*, "Higgs physics at the CLIC electron–positron linear collider", *Eur. Phys. J. C* **77** (2017), article ID 475.
[73] B. Heinemann *et al.*, "Physics Briefing Book: Input for the European Strategy for Particle Physics Update 2020", 2019, preprint, http://cds.cern.ch/record/2691414, https://arxiv.org/abs/1910.11775.
[74] A. Blondel, F. Zimmermann, "A High Luminosity e^+e^- Collider in the LHC tunnel to study the Higgs Boson", 2011, preprint, https://arxiv.org/abs/1112.2518.
[75] U. Amaldi, "A possible scheme to obtain e^-e^- and e^+e^- collisions at energies of hundreds of GeV", *Phys. Lett. B* **61** (1976), no. 3, p. 313-315.
[76] M. Palmer, "Muon collider and neutrino factory", *ICFA Beam Dynamic Newsletter* (2011), no. 55, https://icfa-usa.jlab.org/archive/newsletter/icfa_bd_nl_55.pdf.
[77] R. Palmer, "Muon colliders", *Rev. Accelerator Sci. Technol.* **07** (2014), p. 137-159.
[78] J. P. Delahaye, M. Diemoz, K. Long, B. Mansoulié, N. Pastrone, L. Rivkin *et al.*, "Muon colliders", 2019, preprint, https://arxiv.org/abs/1901.06150.
[79] D. d'Enterria, "Higgs physics at the future circular collider", *PoS* **ICHEP2016** (2017), p. 434.
[80] CMS Collaboration, "Search for a standard model-like Higgs boson in the $\mu^+\,\mu^-$ and e^+e^- decay channels at the LHC", *Phys. Lett. B* **744** (2015), p. 184-207.
[81] ATLAS Collaboration, G. Aad *et al.*, "Search for the Higgs boson decays $H \to ee$ and $H \to e\mu$ in pp collisions at $\sqrt{s} = 13$ TeV with the ATLAS detector", *Phys. Lett. B* **801** (2020), article ID 135148.
[82] J. de Blas *et al.*, "Higgs boson studies at future particle colliders", *JHEP* **01** (2020), article ID 139.
[83] M. McCullough, "An indirect model-dependent probe of the Higgs self-coupling", *Phys. Rev. D* **90** (2014), article ID 015001.
[84] S. Di Vita, G. Durieux, C. Grojean, J. Gu, Z. Liu, G. Panico *et al.*, "A global view on the Higgs self-coupling at lepton colliders", *JHEP* **02** (2018), article ID 178.
[85] F. Maltoni, D. Pagani, X. Zhao, "Constraining the Higgs self couplings at e^+e^- colliders", 2018, preprint, https://arxiv.org/abs/1802.07616.
[86] J. Alison *et al.*, "Higgs boson pair production at colliders: status and perspectives", in *Double Higgs Production at Colliders Batavia, IL, USA, September 4, 2018–9, 2019* (B. Di Micco, M. Gouzevitch, J. Mazzitelli, C. Vernieri, eds.), 2019, https://lss.fnal.gov/archive/2019/conf/fermilab-conf-19-468-e-t.pdf.
[87] A. Blondel, P. Janot, "Future strategies for the discovery and the precise measurement of the Higgs self coupling", 2018, preprint, https://arxiv.org/abs/1809.10041.
[88] P. Janot, "Top-quark electroweak couplings at the FCC-ee", *JHEP* **04** (2015), article ID 182.
[89] V. N. Litvinenko, T. Roser, M. Chamizo-Llatas, "High-energy high-luminosity e^+e^- collider using energy-recovery linacs", *Phys. Lett. B* **804** (2020), article ID 135394.
[90] N. Chakrabarty *et al.*, "Radiative return for heavy Higgs boson at a muon collider", *Phys. Rev. D* **91** (2015), article ID 015008.
[91] E. Eichten, A. Martin, "The muon collider as a H/A factory", *Phys. Lett. B* **728** (2014), p. 125-130.
[92] M. Worek, "Higgs CP from $H/A0 \to \tau\tau$ decay", *Acta Phys. Polon. B* **34** (2003), p. 4549-4560.

[93] A. Blondel, P. Janot, "Circular and linear e^+e^- colliders: another story of complementarity", 2019, preprint, https://arxiv.org/abs/1912.11871.